

Original Article

Application of ^{18}F -FDG PET and diffusion weighted imaging (DWI) in multiple myeloma: comparison of functional imaging modalities

Christos Sachpekidis^{1*}, Jennifer Mosebach^{2*}, Martin T Freitag², Thomas Wilhelm², Elias K Mai³, Hartmut Goldschmidt³, Uwe Haberkorn⁴, Heinz-Peter Schlemmer², Stefan Delorme², Antonia Dimitrakopoulou-Strauss¹

¹Clinical Cooperation Unit Nuclear Medicine, German Cancer Research Center (DKFZ), Heidelberg, Germany; ²Department of Radiology, German Cancer Research Center (DKFZ), Heidelberg, Germany; ³Department of Medicine V, University Clinic Heidelberg, Heidelberg, Germany; ⁴Division of Nuclear Medicine, University Clinic Heidelberg, Heidelberg, Germany. *Equal contributors.

Received July 22, 2015; Accepted August 26, 2015; Epub October 12, 2015; Published October 15, 2015

Abstract: Aim of this prospective study was to assess the sensitivity of positron emission tomography (PET) and diffusion-weighted imaging (DWI) in detecting multiple myeloma (MM) lesions, using the well-established morphologic modalities magnetic resonance imaging (MRI) and computed tomography (CT) as the standard of reference (RS). The study included 24 MM patients (15 newly diagnosed, 9 pre-treated). All underwent ^{18}F -FDG PET/CT and whole-body DWI. The findings in PET and DWI were compared to matching imaging findings in combined non-enhanced T1w, fat-saturated T2w (TIRM)- MRI, and low-dose CT. Patient-based analysis revealed that 15/24 patients (10 primary MM, 5 pre-treated) had myeloma lesions according to our RS. PET was positive in 13/24 patients (11 primary MM, 2 pre-treated) and DWI in 18/24 patients (12 primary MM, 6 pre-treated). Lesion-based analysis demonstrated 128 MM lesions, of which PET depicted 60/128 lesions (sensitivity 47%), while DWI depicted 99/128 lesions (sensitivity 77%). Further analysis including only the 15 untreated MM patients revealed a sensitivity of 90% for both PET and DWI and an overall concordance of PET and DWI of 72%. In conclusion, DWI was more sensitive than ^{18}F -FDG PET in detecting myeloma lesions in a mixed population of primary and pre-treated MM patients. However, ^{18}F -FDG PET and DWI demonstrated equivalent sensitivities in the sub-population of primary, untreated MM patients. This higher sensitivity of DWI in pre-treated patients may be due to the fact that ^{18}F -FDG PET becomes negative earlier in the course of treatment in contrary to MRI, in which already treated lesions can remain visible.

Keywords: Multiple myeloma, ^{18}F -FDG PET, DWI

Introduction

Multiple myeloma (MM) is a malignant monoclonal plasma cell disease affecting the bone marrow, eventually leading to bone destruction and soft tissue manifestations. Presence of focal osseous lesions, detected by PET/CT or MRI, has been proven to be of prognostic significance in all stages of the disease [1-5]. Therefore, findings of CT, including low-dose CT, and MRI have been included in the current definition of symptomatic MM [6].

In addition to the anatomical lesion description, functional imaging becomes more impor-

tant in tumor characterization. Diffusion-weighted imaging (DWI) is a functional MRI technique measuring movement of water molecules within tissues and, thus, providing information regarding microstructure and architecture without the use of contrast agents [7, 8]. Tumor cellularity is known to be a highly influencing parameter regarding the intensity of the DWI signal [9, 10]. Because of their high cellularity, focal MM bone marrow lesions can cause diffusion restriction and show enhanced signal intensity on DWI [11]. If applied in a whole body protocol, all regions of the skeletal system can be surveyed for bone marrow infiltration for staging as well as for monitoring treatment

PET and DWI in multiple myeloma

Table 1. Characteristics of the newly diagnosed and pre-treated MM patients and treatment response according to European Group for Blood and Marrow Transplantation Criteria

Primary/ Pre-treated	Durie/Salmon stage	Sex (M/F)	Age	¹⁸ F-FDG PET uptake pattern	Infiltration pattern MRI	Type of treatment	Time of treatment before scan (months)	Treatment response
Primary	I	M	60	mixed	mixed			
Primary	I	M	64	negative	negative			
Primary	I	M	44	focal	focal			
Primary	I	M	65	mixed	mixed			
Primary	I	F	47	mixed	mixed			
Primary	I	F	53	diffuse	diffuse			
Primary	I	F	64	diffuse	diffuse			
Primary	II	M	55	mixed	mixed			
Primary	II	M	66	mixed	diffuse			
Primary	III	M	78	mixed	mixed			
Primary	III	M	49	focal	mixed			
Primary	III	F	59	mixed	mixed			
Primary	III	F	72	negative	mixed (salt and pepper)			
Primary	III	F	53	focal	mixed			
Primary	III	F	46	mixed	diffuse			
Pre-treated	I	M	58	negative	mixed (hematopoietic marrow possible)	Local radiotherapy	7	
Pre-treated	III	M	70	mixed	mixed	ASCT+chemo	3	CR
Pre-treated	III	M	38	negative	diffuse (salt and pepper)	ASCT+chemo	4	VGPR
Pre-treated	III	M	73	focal	focal	ASCT+chemo	5	nCR
Pre-treated	III	M	65	negative	negative	ASCT+chemo	8	CR
Pre-treated	III	M	54	negative	negative	ASCT+chemo	3	PR
Pre-treated	III	F	68	diffuse	diffuse	ASCT+chemo	3	PR
Pre-treated	III	F	47	negative	mixed (salt and pepper)	ASCT+chemo	3	nCR
Pre-treated	III	F	42	negative	focal	ASCT+chemo	3	CR

Abbreviations: ASCT-autologous stem cell transplantation; PR-partial response; VGPR-very good partial response; nCR-near complete response; CR-complete response.

response. So far this imaging tool has not been included in the guidelines of the international myeloma working group [12, 13].

PET/CT, on the other hand, is a functional imaging modality reflecting metabolic activity. Increased uptake of the radiotracer ^{18}F -FDG is indicative of viable myeloma [14-17]. However, like in DWI, the depiction of ^{18}F -FDG PET-positive findings is not a single criterion for diagnosis of MM, and routine use of PET/CT outside of clinical trials is not generally recommended yet [6, 18, 19].

Aim of this study was to assess the performance of the functional imaging modalities PET and DWI in MM lesion detection and characterisation. In a multi-modality imaging setting we compared the sensitivity of the respective techniques in comparison to the well-established morphologic imaging standard of MRI and CT.

Materials and methods

Patients

24 patients (14 male, 10 female; mean age 57.9 years) with histopathologically confirmed MM were included in the study. Diagnosis was based on the International Myeloma Working Group criteria valid at the time point of patient recruitment [20]. According to the Durie/Salmon staging system, eight patients had stage I, two patients had stage II, and 14 patients had stage III MM. Fifteen patients were newly diagnosed and had received no previous treatment, whilst nine patients had already undergone therapy. The time between possible treatment and the examination was at least three months. The characteristics of the patients involved in the study are presented in **Table 1**.

All patients underwent ^{18}F -FDG PET/CT and MRI exams involving whole-body DWI. Patients gave written informed consent after the study was fully explained to them. Our study was conducted in accordance to the declaration of Helsinki, with institutional approval by the local ethics committee and the "Bundesamt für Strahlenschutz" (national agency of radiation protection in Germany). Patients with contraindications for MRI as pacemaker, claustrophobia etc. and diabetics were excluded from the study.

Data acquisition

PET/CT: A dedicated PET/CT system (Biograph mCT, S128, Siemens Co., Erlangen, Germany) with an axial field of view of 21.6 cm with True Point and TrueV, operated in a three-dimensional mode was used. The PET detector contained four rings of 48 detector blocks; each detector block consisted of 13×13 lutetium oxyorthosilicate crystals ($4 \times 4 \times 20$ mm). Examinations were performed without the application of a contrast agent from the skull base to the knees with an image duration of two minutes per bed position for the emission scans. Low-dose CT (120 kV, 30 mA) was utilized for attenuation correction of the PET data and for image fusion. An image matrix of 400×400 pixels was used for iterative image reconstruction, based on the ordered subset expectation maximization algorithm (OSEM) with six iterations and twelve subsets.

MRI: MRI exams were performed in the framework of PET/MRI studies, directly after the PET/CT studies, making use of the remaining tracer activity. The PET component of the PET/MRI scans was not used for diagnostic purposes; it was applied to visually bridge PET/CT findings to DWI and T1w/T2w on MRI images to achieve a correct matching. An evaluation of the PET-component and SUV-comparison between PET/CT and PET/MRI in 30 patients, which included the patients of this analysis, has been previously reported [21]. A hybrid PET/MRI system (Biograph mMR, Siemens Co., Erlangen, Germany) was used. It consists of a 3.0 Tesla magnet (length, 163 cm; bore size, 60 cm), an actively shielded whole-body gradient coil system (length, 159 cm; amplitude, 45 mT/M; slew rate, 200 T/m/s) and a radiofrequency body coil (peak power, 35 kW; transmitter bandwidth, 800 kHz) [22]. The PET detector contained eight rings of 56 detector blocks; each detector block consisted of 8×8 lutetium oxyorthosilicate crystals ($4 \times 4 \times 20$ mm).

MRI studies were performed without contrast agent from the skull to the mid-thigh including coronal T1w turbo-spin-echo, coronal T2w turbo-inversion-recovery-magnitude, sagittal T1w turbo-spin-echo (TSE) plus T2w turbo-spin-echo-sequences, as well as axial DWI (**Table 2**). PET data were reconstructed with an iterative 3-D OSEM algorithm with two iterations, 21 subsets and an image matrix of 172 pixels. During the PET acquisition a two-point Dixon

PET and DWI in multiple myeloma

Table 2. MR Imaging Parameters, exemplarily of sections with the longest acquisition time

Parameter	T1w TSE cor	T2w TIRM cor	T1w TSE sag	T2w TSE sag	DWI
Orientation	coronal	coronal	sagittal	sagittal	transversal
Slices	38	45	20	21	30
Slice thickness (mm)	5.0	5.0	3.0	3.0	6.0
Distance factor	10%	10%	10%	10%	0%
Voxel size (mm)	2.0×1.4×5.0	2.0×1.4×5.0	1.2×0.9×3.0	1.2×0.9×3.0	3.0×3.0×6.0
Matrix	320×224	320×224	320×243	320×256	134×134
Field of view (cm)	450	450	280	300	400
Repetition time (msec)	800	3050	1050	4560	13300
Echotime (msec)	9.4	76.0	8.9	88.0	68
Turbo/ EPI factor	1	25	5	21	92
Acquisition time per block (min)	3:02	3:28	1:53	2:50	4:13
Imaging blocks	5/5	4/5	1/3	3/3	3-5, depending on patient size
Total acquisition time all blocks/min	8:27	11:10	5:33	7:21	12:39

Abbreviations: cor-coronal; DWI-diffusion weighted imaging; sag-sagittal; TIRM-turbo inversion recovery magnitude, TSE-turbo spin echo; w-weighted. The total acquisition time was 45 minutes 10 seconds for MR including DWI.

volume interpolated breath-hold examination (VIBE) sequence was performed and used for attenuation correction of the PET images.

For diffusion-weighted imaging an axial 2D echoplanar diffusion sequence with three gradient directions and two b-values (0, 800 s/mm²) was applied and used for additional apparent-diffusion-coefficient (ADC)-map calculation as well as reconstruction of rotated and coronal maximum-intensity-projection (MIP)-images (for details see also **Table 2**).

Data analysis

Visual analysis for myeloma suspicious foci was performed by evaluating the transaxial, coronal, and sagittal images of the patients separately for each applied modality by two nuclear medicine physicians and two radiologists on a lesion by lesion basis. Matching was performed in consensus reading using the dedicated imaging software ayacan OsiriX^{PRO}.

Focal myeloma infiltrates: Standard of reference: Since, obviously, histological proof could not be obtained for every lesion, the synopsis of imaging findings in non-enhanced T1w/T2w MRI as well as low-dose CT served as the standard of reference (reference standard, RS) for this study. In certain defined cases lesions were also considered present despite being divergent in MRI and CT, e.g. a typical myeloma lesion in MRI without corresponding lytic bone destruction on low-dose CT, or, vice versa, osteolysis on CT without explicit MRI correlate.

Investigation proceeded according to the following functional and morphological criteria: Low-dose CT: Circumscribed osteolytic lesions (>5 mm diameter) were considered as indicative for MM.

Morphologic MRI: Focal myeloma infiltration was defined by circumscribed areas of high signal intensity on gradient echo and T2w fat-suppressed sequences, such as turbo inversion recovery magnitude (TIRM) images. These corresponded to areas of low signal intensity, or in a few cases isointense signal, on unenhanced T1-weighted TSE images [23, 24].

PET: Skeletal foci presenting with significantly enhanced ¹⁸F-FDG uptake as compared to the surrounding tissue in PET/CT studies were considered suspicious of myeloma in absence of a possible benign etiology (trauma, inflammation, degenerative changes, arthritic disease etc.).

DWI: Signal elevations on DWI b800 images that were displayed on at least three or more slices were included in the study and matched to the findings in the other modalities. DWI-signal in degenerative prone locations (ilio-sacral, facet joint, costo-sternal joint) or extra-osseous DWI-hyperintensities with benign correlate (like in lymph nodes, vessels or muscle) in MRI or CT were not counted. The comparison with PET included only the body areas examined by both imaging modalities (skull to mid-thigh).

Table 3. Patient-based analysis

Parameter	reference standard (CT, MRI)	PET	DWI
No. of primary MM patients with focal lesions	10	11	12
No. of pre-treated MM patients with focal lesions	5	2	6

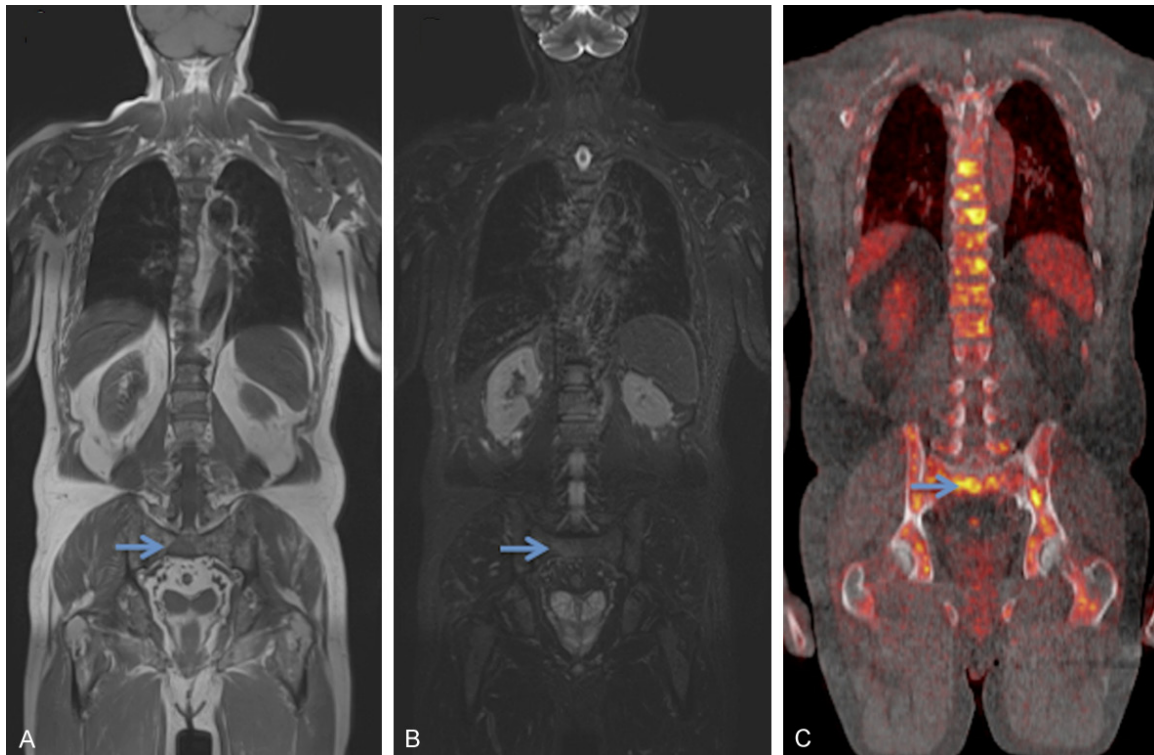


Figure 1. A 66-years old male stage II primary MM patient presenting with a mixed infiltration pattern in MRI (A, T1w; B, T2w TIRM) and a mixed pattern of ^{18}F -FDG uptake in PET (C). The arrows indicate a focal lesion in os sacrum. Multiple focal lesions in the spine are also demonstrated.

General infiltration pattern: Four patterns of ^{18}F -FDG distribution were identified on PET/CT scans: a) negative pattern without any pathological tracer accumulation indicative for MM involvement, b) focal pattern, in which bone marrow foci of increased ^{18}F -FDG uptake were considered MM lesions, c) diffuse pattern, with an “intense”, diffuse bone marrow tracer uptake in maximum intensity projection (MIP) images (compared to tracer accumulation in the spleen [4]), without any ^{18}F -FDG-avid focal lesions, and d) a mixed pattern, in which a combination of diffuse bone marrow uptake and focal bone marrow lesions was detected.

Complementarily, in MRI five different infiltration patterns were described: normal appearing bone marrow, focal infiltration, diffuse infiltration, combined focal and diffuse infiltration, and salt-and-pepper-pattern [25]. Diffuse bone marrow infiltration is characterized by a homo-

geneous decrease of signal on T1w images and increased signal intensity on fat-suppressed T2-weighted images [23, 24]. The salt-and-pepper pattern resembles an intermediate form usually corresponding to a minor infiltration of plasma cells in bone marrow (<20%) [26]. On T1-weighted SE images, but also on gradient echo and T2-weighted SE sequences, the bone marrow appears inhomogeneous but without hyperintense areas in fat saturated sequences [26]. In this study patients were classified into four groups according to their MRI infiltration pattern: a) normal/negative pattern, b) focal pattern, c) diffuse pattern (including salt-and-pepper-pattern), and d) combined focal/diffuse pattern (mixed).

Statistical analysis

The sensitivity of PET and DWI for detection of myeloma lesions was calculated based on the

PET and DWI in multiple myeloma

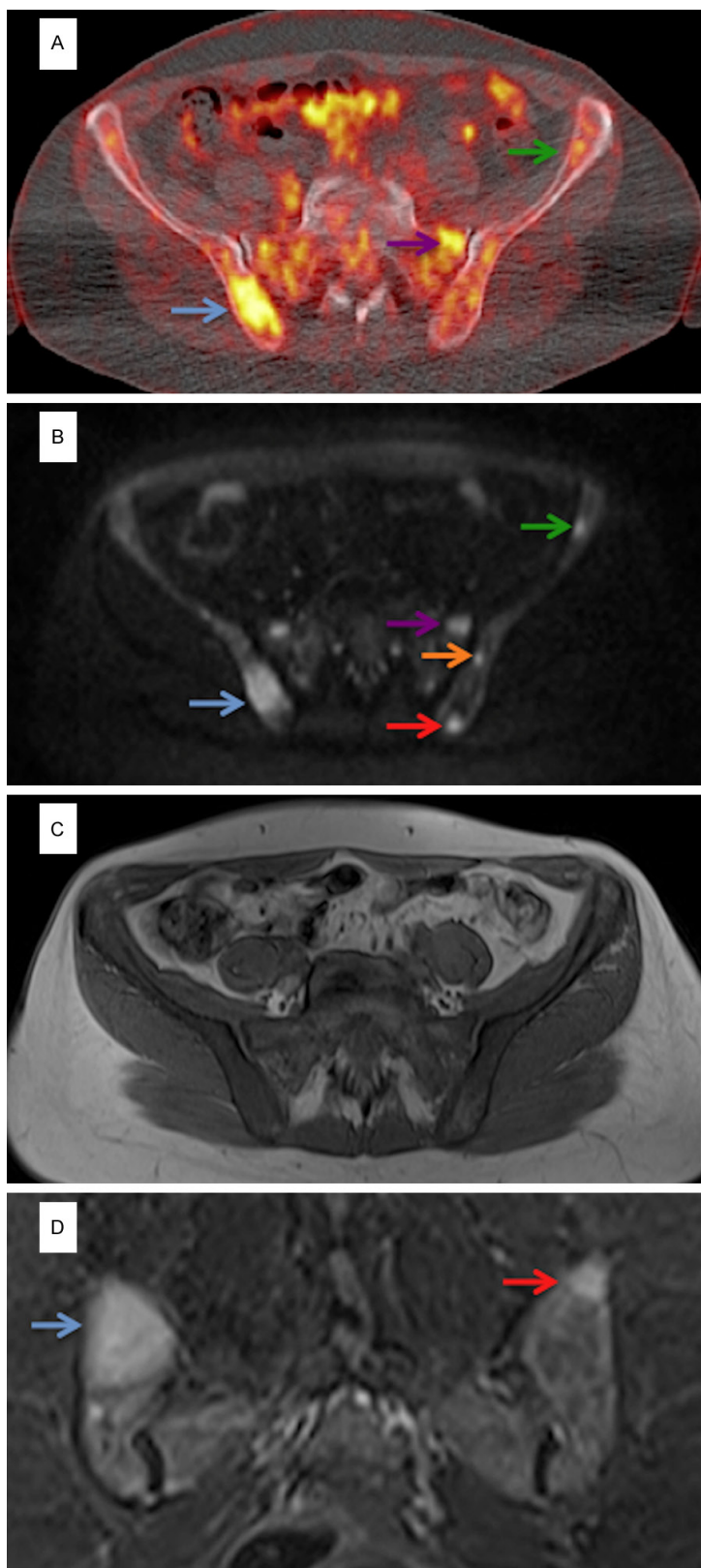


Figure 2. A 53-year old female stage III primary MM patient referred to our department for evaluation of extent of skeletal disease. Transaxial fused PET/CT images at the level of the pelvis (A) reveal a mixed pattern of ¹⁸F-FDG uptake. Corresponding transaxial DWI images (B)

demonstrate also a combination of diffuse infiltration and focal lesions. There is a correlation between some PET- and DWI-positive lesions (blue, purple, green arrows). DWI demonstrates more focal lesions than PET (red, orange arrows), which might be 'masked' by a diffuse ¹⁸F-FDG uptake by the surrounding bone marrow. Transaxial pelvic T1-w MRI (C) exhibits a low bone marrow signal, corresponding to diffuse bone marrow infiltration. In coronal T2-w TIRM (D) two of the lesions depicted in functional imaging modalities are also clearly delineated (arrows).

RS applied for this study (CT and/or MRI findings). Due to the limited number of patients and the heterogeneity with respect to previous therapy, results remain descriptive and testing for statistically significant changes would not have been meaningful in this context.

Results

Patient-based analysis

According to our RS, focal MM lesions could be detected in 15/24 patients (62.5%). Ten of them were untreated on the date of the investigation, while five patients had already received treatment. No malignant lesions could be found in 9/24 patients (37.5%). Benign bone lesions (bone cysts, hemangiomas) were present in 3/24 patients (12.5%), and 19/24 patients (79.2%) presented degenerative joint or bone changes.

In 13/24 patients (54.2%), at least one myeloma indicative lesion was detected by means of ¹⁸F-FDG PET/CT (PET-positive). In particular, eleven patients had primary, previously untreated MM, while two of them had already received therapy in the past. Regarding primary MM patients positive on RS exams (CT and/or MRI), all but one patient

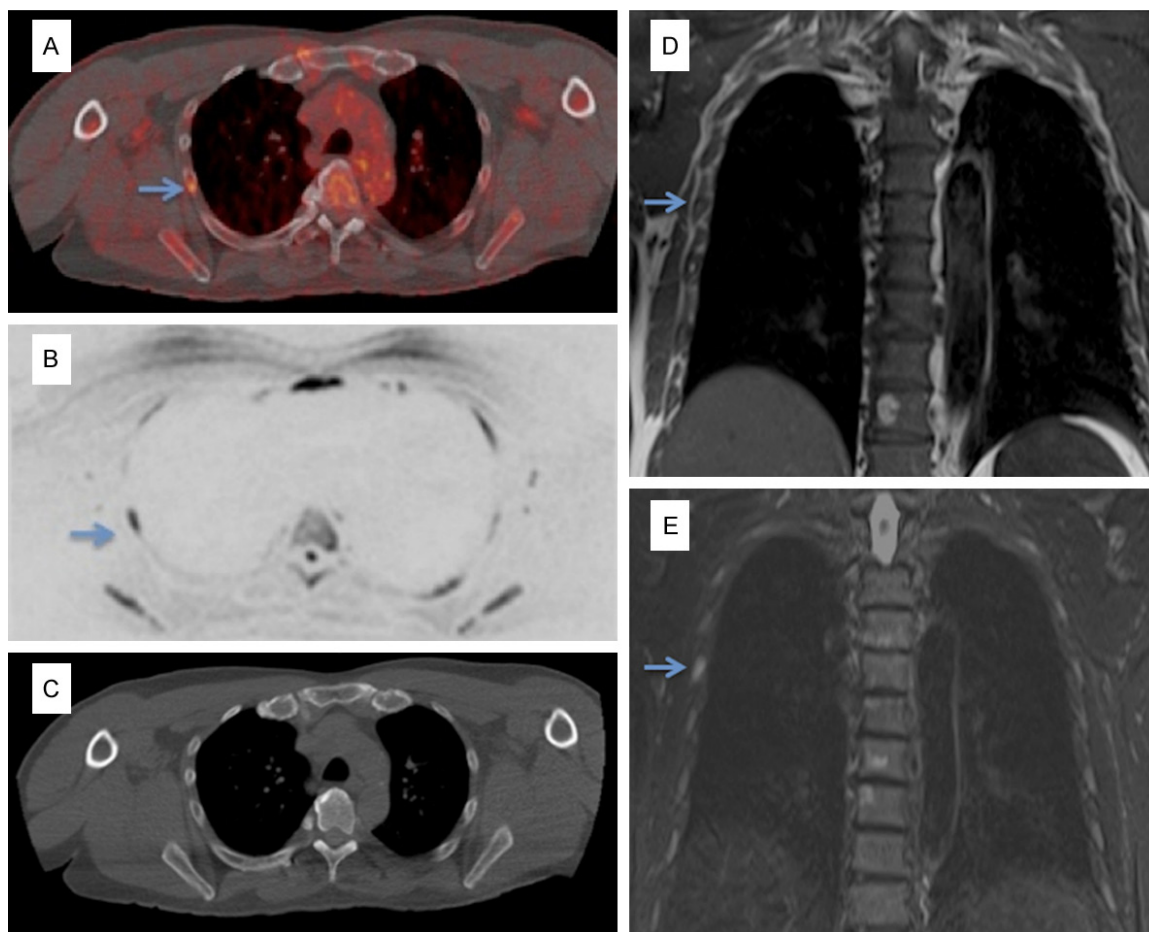


Figure 3. A 65-years old male stage I primary MM patient. Transaxial fused PET/CT images at the thoracic level (A) show a focus of increased ^{18}F -FDG uptake in the 5th right rib dorsolaterally (arrow), which is MM-suspicious. Corresponding DWI images (black/white inverted image, B) also show the rib lesion (arrow). Note diffuse bone marrow infiltration mainly in the sternum and scapulae, depicted with both functional imaging modalities. Transaxial low-dose CT at the same level (C) as well as coronal T1-w MRI (D) and T2-w TIRM MRI (E) show no clear bone destruction or lesion.

were also PET-positive. Two patients were PET-positive and RS-negative. Only 2/5 RS-positive, pretreated patients were PET-positive.

Regarding DWI studies, 18 patients (twelve primary MM, six pre-treated MM) were DWI-positive. All 15 RS-positive patients were also DWI-positive. The two PET-positive and RS-negative patients were DWI-positive (**Table 3**). One patient would have been overdiagnosed in DWI without morphologic imaging because of signal elevation due to bone hemangiomas.

General infiltration pattern

Diffuse ^{18}F -FDG PET bone marrow uptake patterns and infiltration patterns in MRI were com-

parable in 17/24 cases (example shown in **Figure 1**). Three patients with a 'salt and pepper' pattern in MRI showed no pathological diffuse ^{18}F -FDG uptake (see **Table 1**).

Lesion-based analysis

In total 143 lesions were detected with at least one method. According to the RS (CT-, MRI-positive findings), 128 lesions were considered indicative for MM (**Figure 2**). We saw fifteen lesions depicted only on functional imaging modalities (PET, DWI) but not on reference images and counted them as "false positive". In particular, PET detected eight "false positive" (six lesions located in the ribs, two in the pelvis), and DWI yielded nine "false positive" lesions, which proved to be fractures

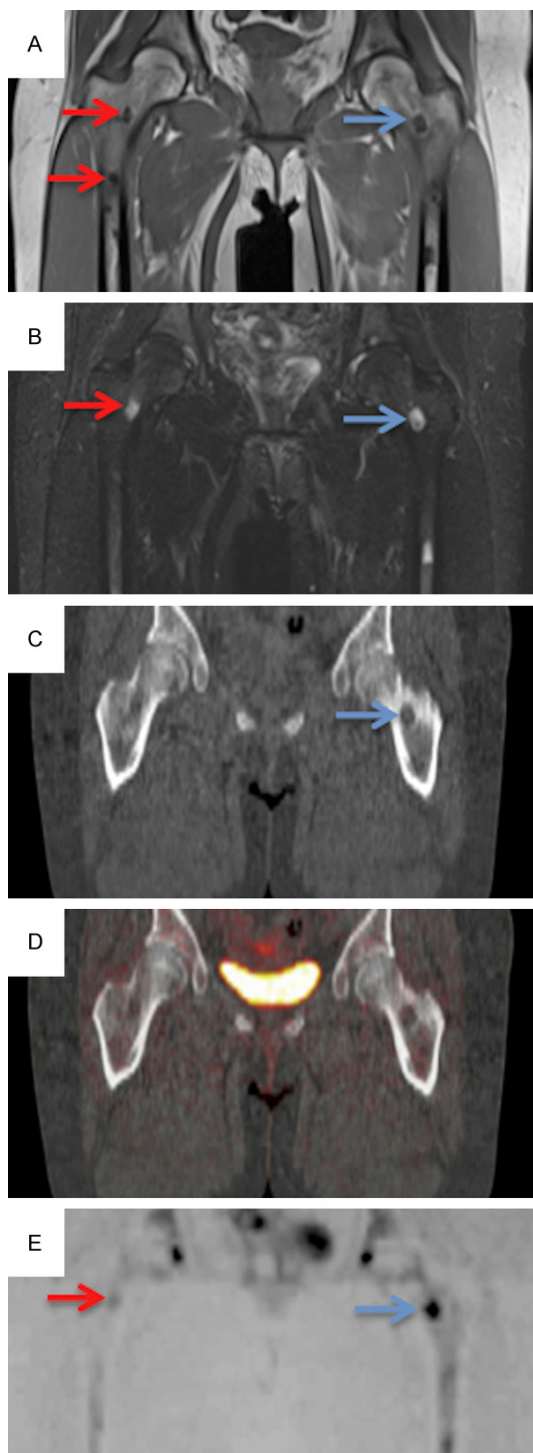


Figure 4. A 47-year old female patient stage III, pre-treated with high-dose chemotherapy and ASCT. Coronal T1w (A), T2w TIRM (B) and CT (C) show multiple lesions in both femurs (arrows). ^{18}F -FDG PET (D) is clearly negative (mismatch). On the other hand, DWI (black/white inverted image, E) is also positive but misses some of the lesions depicted in RS.

(n=2), hemangiomas (n=4) and a ganglion cyst (n=1). Two “false-positive” PET lesions,

located in the anatomic area of the ribs, correlated with respective DWI-findings.

Figure 2 shows a primary, untreated MM patient positive on both RS (CT, MRI) and functional (PET, DWI) imaging modalities. **Figure 3** shows also a primary, untreated MM patient, who was positive for MM on the functional modalities but negative on RS. **Figures 4, 5** show two pre-treated MM patients as examples for mismatch between PET imaging findings and RS/DWI findings. In particular, the patient in **Figure 4** shows multiple focal myeloma lesions on RS and DWI, while PET shows no lesions. The patient in **Figure 5** demonstrates diffuse bone marrow infiltration on MRI and DWI, but there is no pathological ^{18}F -FDG bone marrow uptake on PET. **Figure 6** shows a patient with myeloma lesions visible on T1-w and T2-w sequences but not on DWI due to limitations of DWI regarding field of view.

Regarding lesions detected with RS but not with functional imaging modalities, there were 68 false-negative findings in PET, and 29 in DWI. Sensitivities for MM lesions (according to RS) were 60/128 (47%) for PET and 99/128 (77%) for DWI (**Figure 7**). Corresponding detection qualities of PET and DWI were seen in 81/143 (57%) of all lesions.

We performed a further analysis including only untreated patients. In this, both PET and DWI had a sensitivity of 90% (57/63 lesions) (**Figure 7**). PET and DWI were in agreement in 55/76 lesions (72%) and divergent in the remaining 21 lesions (28%).

Discussion

We aimed to assess the sensitivity of the functional imaging modalities ^{18}F -FDG PET and DWI in detecting myelomatous lesions, using the well-established modalities MRI and/or CT as the standard of reference (RS). The assessment of both primary and pre-treated MM patients revealed that the sensitivity of DWI (77%) was higher than that of ^{18}F -FDG PET (47%). In patient-based analysis, all DWI positive patients were also positive according to the reference standard.

^{18}F -FDG PET was negative in 68 of the 128 RS-positive lesions (53%) (examples seen in **Figure 4**). The majority of these “false negative” lesions (62/68=91%) was found in five patients, who had previously been treated. In particular,

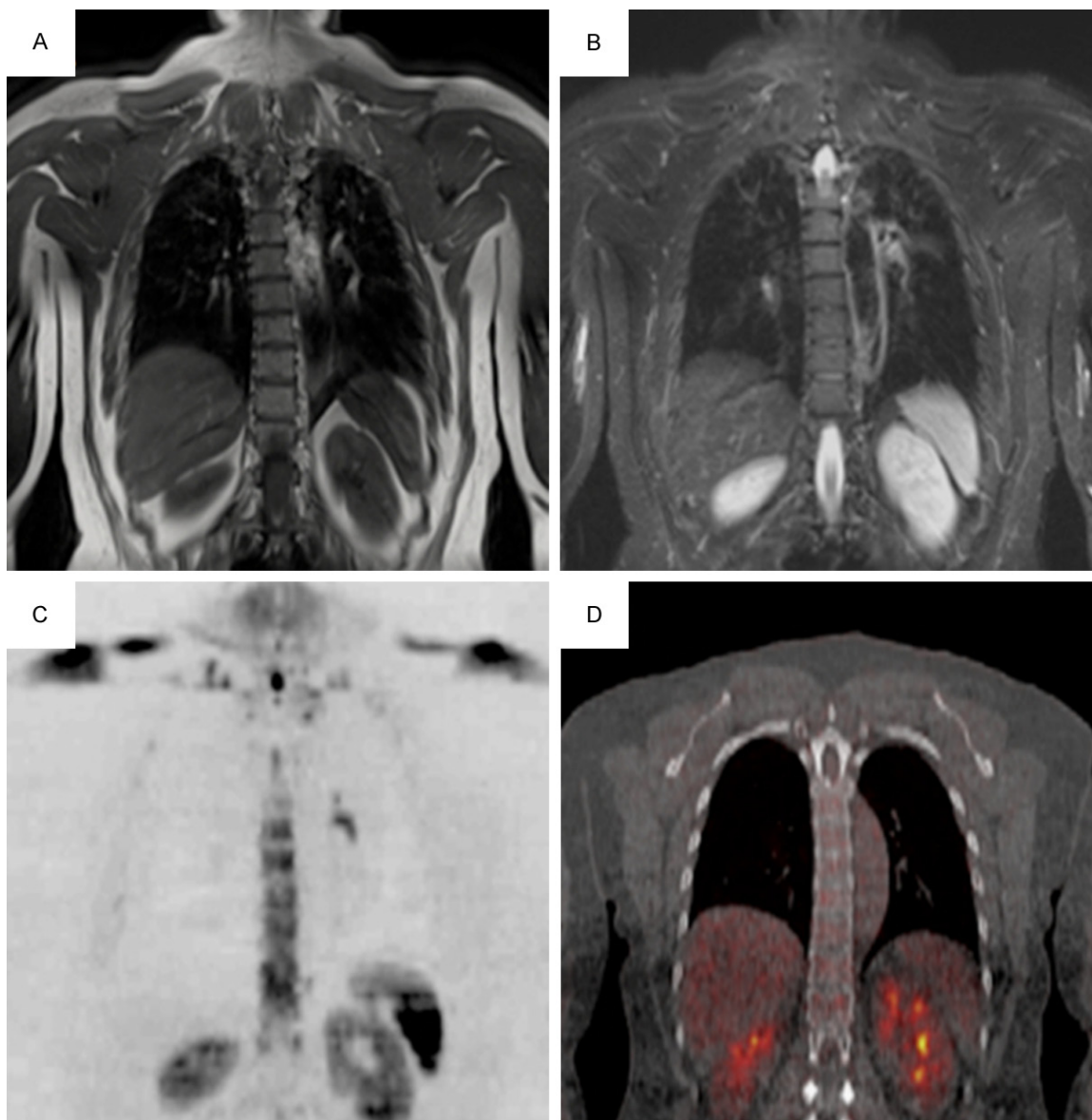


Figure 5. Diffuse bone marrow infiltration demonstrated on T1w (low signal) (A), T2w TIRM (B) and DWI (black/white inverted image, C). Negative pattern of ^{18}F -FDG bone marrow uptake on PET (D). Same patient shown as in **Figure 4**.

four of these patients had received high-dose chemotherapy and autologous stem cell transplantation (ASCT; mean interval=95 days after the end of treatment). The patients' response, according to the International Uniform Response Criteria, had been stated as near complete response (nCR, n=2) and complete response (CR, n=2) [27]. The fifth patient (stage I) had received local radiation therapy of the pelvis seven months before the study (**Table 1**).

A mismatch between ^{18}F -FDG PET and anatomic imaging modalities regarding demonstration

of MM lesions early in the course of treatment has previously been described elsewhere [28]. Due to its ability to differentiate between vital and fibrotic lesions [5] and to the fact that glucose metabolism is a sensitive parameter that decreases earlier in the course of chemotherapy than tumor size [29], ^{18}F -FDG PET/CT is being recommended for treatment response evaluation in MM as well as in several tumor entities [30, 31]. In terms of ASCT response assessment, previous studies have shown that ^{18}F -FDG PET/CT correlates well with the patient's clinical response and that ^{18}F -FDG

PET and DWI in multiple myeloma



Figure 6. Myeloma lesions in both humeri not visible on DWI (A, black arrows), but visible in morphological MR-sequences as areas of hypointense signal in T1-w (B, white arrows) and as hyperintense areas in T2-w TIRM (C, white arrows).

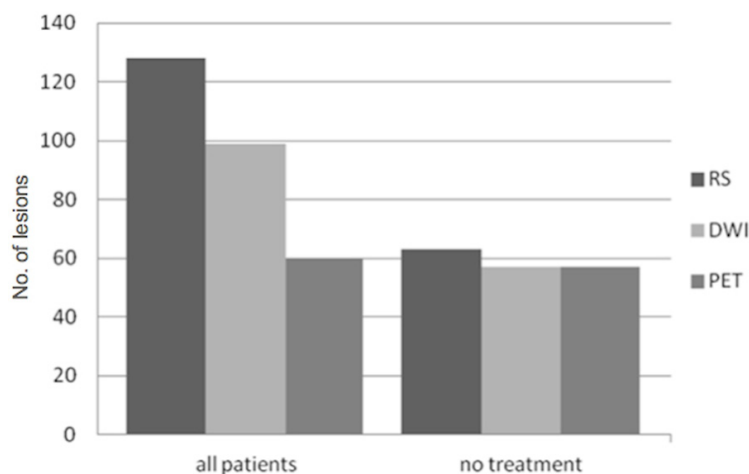


Figure 7. Graph depicting the number of lesions detected with RS, DWI and PET in all MM patients (primary and pre-treated) as well as in the subgroup of primary, untreated MM patients.

Only 9% of RS-positive and PET-negative lesions (6/68) were found in primary MM patients. Five of them were situated inside bone marrow that showed an intense diffuse ^{18}F -FDG uptake, and we, therefore, assume that lesions (in this case 8-13 mm in diameter) might have been masked because the surrounding bone marrow was diffusely infiltrated by myeloma (Figure 2) [5]. The question of dignity regarding primarily labelled “false positive” lesions on PET and/or DWI remains (Figure 3), and could only be solved by direct point-to-point histopathological comparison.

PET suppression precedes normalization in MRI [3, 4, 32, 33]. Nevertheless, MRI is also a valid tool to assess treatment response, because resolution of lesions in MRI after therapy is associated with a favorable prognosis [34, 35], although it takes longer for responding lesions to disappear than in PET [5, 28, 34]. In a recent study involving 21 MM patients undergoing ASCT, the diagnostic performance of whole-body MRI versus PET/CT was compared for determination of remission status after treatment. The authors confirmed that PET/CT remission status correlated significantly with standard response criteria, in contrary to MRI, and they stressed the often-observed false positive findings in MRI, due to non-viable tumor [36].

Failure of DWI to detect 29 lesions can be attributed to several factors. Firstly, some lesions, were located near the margins of the field of view in the whole-body protocol (e.g. humeri, Figure 6), where lesions by experience are often less conspicuous than in the center (10 lesions). Secondly, some lesions were relatively small (<1.5 cm), so that they appeared in only one or two slices (13 lesions); according to our study design, only lesions visible on at least 3 slices were counted as DWI-positive. A third possible mismatch reason was a metal implant causing susceptibility artefacts (1 lesion). Finally, three lesions were potentially masked by a diffuse signal increase of the surrounding bone marrow in DWI. For two RS-positive, DWI-negative lesions located in the spine of one

patient, it is unclear why they were not detectable in DWI.

Nevertheless, DWI is widely regarded as a promising tool for tumor characterization and for prediction of response to treatment. Previous studies comparing DWI at 1.5 T with ^{18}F -FDG PET/CT have shown that the two modalities are comparable for detection of malignant lesions [37, 38]. In our sub-population involving only untreated MM patients, PET and DWI were equally sensitive (90%). Furthermore, all RS-positive primary MM patients were both DWI- and PET-positive, resulting in correct diagnosis by the definition used in this study, except for one patient (one PET-negative lesion located in the scapula).

Regarding the significance of DWI in MM, Giles et al. have recently shown in 20 patients with relapsed MM that whole body DWI detects more lesions than radiographic skeletal survey [39]. Moreover, the DWI-derived apparent diffusion coefficient (ADC) as a quantitative parameter for myeloma and bone marrow cellularity could be used for treatment response monitoring [40-43]. Nevertheless, there will always be a trade-off between image quality and the duration of measurements for physical reasons. With whole-body protocols, one will not be able to achieve the same image quality as when examining only one body region if the scan time is to remain acceptable for the patient. Our investigations emphasise the importance of combined morphologic and functional imaging in the evaluation of myeloma patients, since singular functional imaging would underestimate the number of lesions especially after previous treatment.

This study has some limitations. Firstly, the cohort of patients studied is small. Therefore, the presented results can only be considered as the preliminary results of an ongoing study. Another limitation lies in the heterogeneity of the population studied, which included both newly diagnosed and previously treated patients without baseline imaging. Obviously, histological confirmation of every PET-positive and DWI-positive lesion is impossible in clinical practice and, therefore, lesions need to be compared to a RS. Here, we used a commonly accepted imaging-based RS, which was adapted to established criteria using whole-body T1w-/T2w-MR and CT imaging. In fact, PET and

DWI detected additional lesions, indicating that the RS is not perfect and might miss findings. Therefore, our study provides evidence that the obtained information from DWI and PET compared to T1w and T2w sequences is not redundant but complementary. The question remains, whether RS-negative but PET/DWI-positive findings represent focal myeloma lesions or not, which cannot be answered by the present study due to the lack of lesion-based histopathological ground truth. Future studies assessing this topic, ideally employing hybrid PET/MRI with isocentric acquisitions of both MRI and PET, are needed to elucidate this question.

Conclusion

The present study shows that DWI detects more foci of myeloma than ^{18}F -FDG PET in a mixed population of primary and pre-treated MM patients, compared to the well-established imaging standard of MRI and CT as reference. This mismatch between PET and DWI findings was mainly seen in pre-treated patients and the RS-positive/PET-negative lesions corresponded to the DWI-positive/PET-negative lesions. Given the fact that response to treatment on morphological images (as MRI) does not occur as early as on ^{18}F -FDG PET/CT and, considering the patients' clinical response (nCR, CR), it is possible that the PET-negative lesions that are depicted on RS and DWI may in fact be false-positives because they do not represent viable tumor tissue [44]. The two functional modalities (PET, DWI) are equally sensitive in the sub-population of primary, untreated MM patients. DWI, applied in a whole-body protocol, still has limitations regarding field of view or resolution, rendering, therefore, morphologic imaging mandatory. Further prospective clinical trials will be needed to specify the role of MRI/DWI and PET, regarding the gain in information, duration of exam, and costefficiency.

Disclosure of conflict of interest

None.

Address correspondence to: Dr. Christos Sachpekidis, Medical PET Group-Biological Imaging, Clinical Cooperation Unit Nuclear Medicine, German Cancer Research Center, Im Neuenheimer Feld 280,

PET and DWI in multiple myeloma

D-69210 Heidelberg, Germany. E-mail: christos_saxpe@yahoo.gr; c.sachpekidis@dkfz.de

References

- [1] Hillengass J, Fechtner K, Weber MA, Bäuerle T, Ayyaz S, Heiss C, Hielscher T, Moehler TM, Egerer G, Neben K, Ho AD, Kauczor HU, Delorme S, Goldschmidt H. Prognostic significance of focal lesions in whole-body magnetic resonance imaging in patients with asymptomatic multiple myeloma. *J Clin Oncol* 2010; 28: 1606-1610.
- [2] Hillengass J, Weber MA, Kilk K, Listl K, Wagner-Gund B, Hillengass M, Hielscher T, Farid A, Neben K, Delorme S, Landgren O, Goldschmidt H. Prognostic significance of whole-body MRI in patients with monoclonal gammopathy of undetermined significance. *Leukemia* 2014; 28: 174-178.
- [3] Bartel TB, Haessler J, Brown TL, Shaughnessy JD Jr, van Rhee F, Anaissie E, Alpe T, Angtuaco E, Walker R, Epstein J, Crowley J, Barlogie B. F18-fluorodeoxyglucose positron emission tomography in the context of other imaging techniques and prognostic factors in multiple myeloma. *Blood* 2009; 114: 2068-2076.
- [4] Zamagni E, Patriarca F, Nanni C, Zannetti B, Englaro E, Pezzi A, Tacchetti P, Buttignol S, Perrone G, Brioli A, Pantani L, Terragna C, Carobolante F, Baccarani M, Fanin R, Fanti S, Cavo M. Prognostic relevance of 18-F FDG PET/CT in newly diagnosed multiple myeloma patients treated with up-front autologous transplantation. *Blood* 2011; 118: 5989-5995.
- [5] Zamagni E, Cavo M. The role of imaging techniques in the management of multiple myeloma. *Br J Haematol* 2012; 159: 499-513.
- [6] Rajkumar SV, Dimopoulos MA, Palumbo A, Blade J, Merlini G, Mateos MV, Kumar S, Hillengass J, Kastiris E, Richardson P, Landgren O, Paiva B, Dispenzieri A, Weiss B, LeLeu X, Zweegman S, Lonial S, Rosinol L, Zamagni E, Jagannath S, Sezer O, Kristinsson SY, Caers J, Usmani SZ, Lahuerta JJ, Johnsen HE, Beksac M, Cavo M, Goldschmidt H, Terpos E, Kyle RA, Anderson KC, Durie BG, Miguel JF. International Myeloma Working Group updated criteria for the diagnosis of multiple myeloma. *Lancet Oncol* 2014; 15: e538-e548.
- [7] Horger M, Weisel K, Horger W, Mroue A, Fenchel M, Lichy M. Whole-body diffusion-weighted MRI with apparent diffusion coefficient mapping for early response monitoring in multiple myeloma: preliminary results. *AJR Am J Roentgenol* 2011; 196: W790-795.
- [8] Charles-Edwards EM, deSouza NM. Diffusion-weighted magnetic resonance imaging and its application to cancer. *Cancer Imaging* 2006; 6: 135-143.
- [9] Le Bihan D, Breton E, Lallemand D, Aubin ML, Vignaud J, Laval-Jeantet M. "Separation of diffusion and perfusion in intravoxel incoherent motion MR imaging. *Radiology* 1988; 168: 497-505.
- [10] Le Bihan DJ. Differentiation of benign versus pathologic compression fractures with diffusion-weighted MR imaging: a closer step toward the "holy grail" of tissue characterization? *Radiology* 1998; 207: 305-307.
- [11] Lin C, Itti E, Luciani A, Haioun C, Meignan M, Rahmouni A. Whole-body diffusion-weighted imaging in lymphoma. *Cancer Imaging* 2010; 10 Spec no A: S172-178.
- [12] Xu X, Ma L, Zhang JS, Cai YQ, Xu BX, Chen LQ, Sun F, Guo XG. Feasibility of whole body diffusion weighted imaging in detecting bone metastasis on 3.0T MR scanner. *Chin Med Sci J* 2008; 23: 151-157.
- [13] Padhani AR, Koh DM. Diffusion MR imaging for monitoring of treatment response. *Magn Reson Imaging Clin N Am* 2011; 19: 181-209.
- [14] Durie BG, Waxman AD, D'Agnolo A, Williams CM. Whole-body (18)F-FDG PET identifies high-risk myeloma. *J Nucl Med* 2002; 43: 1457-1463.
- [15] Schirrmeister H, Bommer M, Buck AK, Müller S, Messer P, Bunjes D, Döhner H, Bergmann L, Reske SN. Initial results in the assessment of multiple myeloma using 18F-FDG PET. *Eur J Nucl Med Mol Imaging* 2002; 29: 361-366.
- [16] Durie BG. The role of anatomic and functional staging in myeloma: description of Durie/Salmon plus staging system. *Eur J Cancer* 2006; 42: 1539-1543.
- [17] van Lammeren-Venema D, Regelink JC, Riphagen II, Zweegman S, Hoekstra OS, Zijlstra JM. 18F-fluoro-deoxyglucose positron emission tomography in assessment of myeloma-related bone disease: a systematic review. *Cancer* 2012; 118: 1971-1981.
- [18] Bird JM, Owen RG, D'Sa S, Snowden JA, Pratt G, Ashcroft J, Yong K, Cook G, Feyler S, Davies F, Morgan G, Cavenagh J, Low E, Behrens J; Haemato-oncology Task Force of British Committee for Standards in Haematology (BCSH) and UK Myeloma Forum. Guidelines for the diagnosis and management of multiple myeloma. *Br J Haematol* 2011; 154: 32-75.
- [19] Dimopoulos M, Kyle R, Ferman J, Rajkumar SV, San Miguel J, Chanan-Khan A, Ludwig H, Joshua D, Mehta J, Gertz M, Avet-Loiseau H, Beksaç M, Anderson KC, Moreau P, Singhal S, Goldschmidt H, Boccadoro M, Kumar S, Giralt S, Munshi NC, Jagannath S; International Myeloma Workshop Consensus Panel 3. Consensus recommendations for standard in-

PET and DWI in multiple myeloma

- vestigative workup: report of the International Myeloma Workshop Consensus Panel 3. *Blood* 2011; 117: 4701-4705.
- [20] International Myeloma Working Group. Criteria for the classification of monoclonal gammopathies, multiple myeloma and related disorders: a report of the International Myeloma Working Group. *Br J Haematol* 2003; 121: 749-757.
- [21] Sachpekidis C, Hillengass J, Goldschmidt H, Mosebach J, Pan L, Schlemmer HP, Haberkorn U, Dimitrakopoulou-Strauss A. Comparison of 18F-FDG PET/CT and PET/MRI in patients with multiple myeloma. *Am J Nucl Med Mol Imaging* (accepted for publication).
- [22] Delso G, Fürst S, Jakoby B, Ladebeck R, Ganter C, Nekolla SG, Schwaiger M, Ziegler SI. Performance measurements of the Siemens mMR integrated whole-body PET/MR scanner. *J Nucl Med* 2011; 52: 1914-1922.
- [23] Rahmouni A, Divine M, Mathieu D, Golli M, Dao TH, Jazaerli N, Anglade MC, Reyes F, Vasile N. Detection of multiple myeloma involving the spine: efficacy of fat-suppression and contrast-enhanced MR imaging. *AJR Am J Roentgenol* 1993; 160: 1049-1052.
- [24] Baur-Melnyk A, Buhmann S, Dürr HR, Reiser M. Role of MRI for the diagnosis and prognosis of multiple myeloma. *Eur J Radiol* 2005; 55: 56-63.
- [25] Baur A, Stäbler A, Bartl R, Lamerz R, Reiser M. Infiltration patterns of plasmacytomas in magnetic resonance tomography. *Rofo* 1996; 164: 457-463.
- [26] Baur-Melnyk A, Buhmann S, Dürr HR, Reiser M. Role of MRI for the diagnosis and prognosis of multiple myeloma. *Eur J Radiol* 2005; 55: 56-63.
- [27] Durie BG, Harousseau JL, Miguel JS, Bladé J, Barlogie B, Anderson K, Gertz M, Dimopoulos M, Westin J, Sonneveld P, Ludwig H, Gahrton G, Beksac M, Crowley J, Belch A, Boccadaro M, Cavo M, Turesson I, Joshua D, Vesole D, Kyle R, Alexanian R, Tricot G, Attal M, Merlini G, Powles R, Richardson P, Shimizu K, Tosi P, Morgan G, Rajkumar SV; International Myeloma Working Group. International uniform response criteria for multiple myeloma. *Leukemia* 2006; 20: 1467-1473.
- [28] Caers J, Withofs N, Hillengass J, Simoni P, Zamagni E, Hustinx R, Beguin Y. The role of positron emission tomography-computed tomography and magnetic resonance imaging in diagnosis and follow up of multiple myeloma. *Haematologica* 2014; 99: 629-637.
- [29] Juweid ME, Cheson BD. Positron-emission tomography and assessment of cancer therapy. *N Engl J Med* 2006; 354: 496-507.
- [30] Wahl RL, Jacene H, Kasamon Y, Lodge MA. From RECIST to PERCIST: Evolving Considerations for PET response criteria in solid tumors. *J Nucl Med* 2009; 50 Suppl 1: 122S-150S.
- [31] Dimitrakopoulou-Strauss A. PET-based molecular imaging in personalized oncology: potential of the assessment of therapeutic outcome. *Future Oncol* 2015; 11: 1083-1091.
- [32] Zamagni E, Nanni C, Patriarca F, Englaro E, Castellucci P, Geatti O, Tosi P, Tacchetti P, Cangini D, Perrone G, Ceccolini M, Brioli A, Buttignol S, Fanin R, Salizzoni E, Baccarani M, Fanti S, Cavo M. A prospective comparison of 18F-fluorodeoxyglucose positron emission tomography-computed tomography, magnetic resonance imaging and whole-body planar radiographs in the assessment of bone disease in newly diagnosed multiple myeloma. *Haematologica* 2007; 92: 50-55.
- [33] Dimitrakopoulou-Strauss A, Hoffmann M, Bergner R, Uppenkamp M, Haberkorn U, Strauss LG. Prediction of progression-free survival in patients with multiple myeloma following anthracycline-based chemotherapy based on dynamic FDG-PET. *Clin Nucl Med* 2009; 3: 576-584.
- [34] Walker R, Barlogie B, Haessler J, Tricot G, Anaissie E, Shaughnessy JD Jr, Epstein J, van Hemert R, Erdem E, Hoering A, Crowley J, Ferris E, Hollmig K, van Rhee F, Zangari M, Pineda-Roman M, Mohiuddin A, Yaccoby S, Sawyer J, Angtuaco EJ. Magnetic resonance imaging in multiple myeloma: diagnostic and clinical implications. *J Clin Oncol* 2007; 25: 1121-1128.
- [35] Hillengass J, Ayyaz S, Kilk K, Weber MA, Hielscher T, Shah R, Hose D, Delorme S, Goldschmidt H, Neben K. Changes in magnetic resonance imaging before and after autologous stem cell transplantation correlate with response and survival in multiple myeloma. *Haematologica* 2012; 97: 1757-1760.
- [36] Derlin T, Peldschus K, Münster S, Bannas P, Herrmann J, Stübiger T, Habermann CR, Adam G, Kröger N, Weber C. Comparative diagnostic performance of 18F-FDG PET/CT versus whole-body MRI for determination of remission status in multiple myeloma after stem cell transplantation. *Eur Radiol* 2013; 23: 570-578.
- [37] Komori T, Narabayashi I, Matsamura K, Matsuki M, Akagi H, Ogura Y, Aga F, Adachi I. 2-[Fluorine-18]-fluoro-2-deoxy-D-glucose positron emission tomography/computed tomography versus whole-body diffusion-weighted MRI for detection of malignant lesions: initial experience. *Ann Nucl Med* 2007; 21: 209-215.
- [38] Lichy MP, Aschoff P, Plathow C, Stemmer A, Horger W, Mueller-Horvat C, Steidle G, Horger M, Schafer J, Eschmann SM, Kiefer B, Claussen CD, Pfannenberger C, Schlemmer HP. Tumor de-

PET and DWI in multiple myeloma

- tection by diffusion-weighted MRI and ADC-mapping—initial clinical experiences in comparison to PET-CT. *Invest Radiol* 2007; 42: 605-613.
- [39] Giles SL, deSouza NM, Collins DJ, Morgan VA, West S, Davies FE, Morgan GJ, Messiou C. Assessing myeloma bone disease with whole-body diffusion-weighted imaging: comparison with x-ray skeletal survey by region and relationship with laboratory estimates of disease burden. *Clin Radiol* 2015; 70: 614-21.
- [40] Hillengass J, Bäuerle T, Bartl R, Andrulis M, McClanahan F, Laun FB, Zechmann CM, Shah R, Wagner-Gund B, Simon D, Heiss C, Neben K, Ho AD, Schlemmer HP, Goldschmidt H, Delorme S, Stieltjes B. Diffusion-weighted imaging for non-invasive and quantitative monitoring of bone marrow infiltration in patients with monoclonal plasma cell disease: a comparative study with histology. *Br J Haematol* 2011; 153: 721-728.
- [41] Horger M, Weisel K, Horger W, Mroue A, Fenchel M, Lichy M. Whole-body diffusion-weighted MRI with apparent diffusion coefficient mapping for early response monitoring in multiple myeloma: preliminary results. *AJR Am J Roentgenol* 2011; 196: W790-795.
- [42] Messiou C, Giles S, Collins DJ, West S, Davies FE, Morgan GJ, Desouza NM. Assessing response of myeloma bone disease with diffusion-weighted MRI. *Br J Radiol* 2012; 85: e1198-1203.
- [43] Giles SL, Messiou C, Collins DJ, Morgan VA, Simpkin CJ, West S, Davies FE, Morgan GJ, deSouza NM. Whole-body diffusion-weighted MR imaging for assessment of treatment response in myeloma. *Radiology* 2014; 271: 785-794.
- [44] Walker RC, Brown TL, Jones-Jackson LB, De Blanche L, Bartel T. Imaging of multiple myeloma and related plasma cell dyscrasias. *J Nucl Med* 2012; 53: 1091-1101.